Nano-Structures & Nano-Objects 25 (2021) 100660

Contents lists available at ScienceDirect

Nano-Structures & Nano-Objects

journal homepage: www.elsevier.com/locate/nanoso

Converting raw coal powder into polycrystalline nano-graphite by metal-assisted microwave treatment

Christoffer A. Masi [a], Teneil A. Schumacher [a,b], Joann Hilman [a], Rabindra Dulal [a], Gaurab Rimal [a,1], Bang Xu [d], Brian Leonard [c], Jinke Tang [a], Maohong Fan [d,e], TeYu Chien [a,*]

[a] Department of Physics & Astronomy, University of Wyoming, Laramie, WY 82071, USA
[b] Department of Chemical Engineering, University of Wyoming, Laramie, WY 82071, USA
[c] Department of Chemistry, University of Wyoming, Laramie, WY 82071, USA
[d] Department of Chemical & Petroleum Engineering, University of Wyoming, Laramie, WY 82071, USA
[e] School of Energy Resources, University of Wyoming, Laramie, WY 82071, USA

ARTICLE INFO

Article history:
Received 21 October 2020
Received in revised form 7 December 2020
Accepted 17 December 2020

Keywords:
Coal
Microwave
Nano-graphite

ABSTRACT

A metal-assisted microwave treatment that converting raw coal powders into nano-graphite is presented. Specifically, four major factors are identified for successful conversion: (1) high temperature; (2) reducing environment; (3) catalyst; and (4) microwave radiation. Specifically, it is determined that the combination of the carbon sources (raw coal powders), the high temperature (microwave induced electric sparking), the reducing environment (the Ar/H_2 mixture), the catalyst (Cu foil), with the microwave radiations can generate nano-graphites. This novel approach utilizes the sparking induced by the microwave radiation on the fork-shape metal foils to generate high temperature (> 1000 °C) within few seconds. The small thermal load makes this method cost effective and has potential for higher temperature using metals with higher melting temperature. Refinement of this technique is possible to yield a higher quality and quantity of nano-graphite materials for a wider range of applications.

1. Introduction

Coal is one of the most available carbon materials worldwide with the United States alone producing 756.2 million tons of Coal in 2018 [1]. Among them, ~90% of the coal is used for electricity generation through combustion, which poses concerns in climate change. While alternative energy sources are actively investigated in order to replace fossil fuels for energy generation, the abundant coal resources will face transitions toward other usages. Thus, converting coal materials into higher value materials, such as graphene, graphite, and/or carbon nanotubes, is of high interests [2]. Among the high value carbon materials, graphite is used in a wide variety of applications, including lubricants [3–5], high-temperature gaskets [4], non-porous sealing layers [4], fire extinguisher agent for metal fires [4], thermal insulators for molten metals [4], conductivity additives for electromagnetic reflectors [6], enhancing mechanical performance [7], synthesizing other carbon materials (including graphene quantum dots (GQDs)) [8,9], graphite intercalation compounds (GICs [4,10]), fuel cells [11], and lithium ion batteries [12,13]. Finite graphite reserves and environmental concerns for the graphite extraction procedures [14,15] make the method of converting coal to graphite a great alternative source of graphite production.

Overall, the molecular structures of coal are complicated [16–18]. The complexity of coal is twofold. First, there are no common molecular structures [19]. Generally, simplified molecular representations contain nm or sub-nm sized crystalline carbon domains with defects that are linked by amorphous carbons [20]. Over one hundred variants of molecular level representations of coal or coal extracts have been reported [21]. Second, coal contains a variety of impurities, either as inorganic [18] and organic parts in both stable and volatile states [22]. Given the complexity, coal conversion is not a trivial task. The feasibility of preparing carbon nanomaterials from coal was first established by Pang et al. with the synthesis of C_{60} and C_{70} [23]. Since then, coal is considered as an important carbon source for synthesizing carbon nanotubes [24–27], and graphene quantum dots (GQDs) [28]. On the other hand, even without purifications and detail characterizations, minimally processed coal was synthesized into a thin film for a joule heating device [29].

Among the various methods used to convert coal into carbon materials, microwave treatments are attractive due to the low cost and high efficiency. Microwaves are electromagnetic

* Corresponding author.
E-mail address: tchien@uwyo.edu (T. Chien).

[1] Current address: Department of Physics and Astronomy, Rutgers University, Piscataway, NJ 08904.

https://doi.org/10.1016/j.nanoso.2020.100660
2352-507X/

waves with a frequency ranging from 300 MHz to 300 GHz. Two frequencies (0.915 and 2.45 GHz) are reserved by the Federal Communications Commission (FCC) for industrial, scientific, medical, and instrumentation (ISMI) purposes [30]. Previous studies have proven microwave radiation effective in treating coal materials. For instance, microwaves were used for measuring moisture content [31,32], dewatering of coals [33–37], removing sulfur and mineral matters from coal [38,39], and converting coal into commercial fuels [40]. Microwave treatments were also used in synthesizing carbon nanoparticles [41] and GQDs [42]. Similarly, graphene oxides produced through a modified Hummers' method on graphite were successfully reduced to high quality graphene via microwave treatment [38]. These reported methods utilize microwaves as a method of fast energy transfer with dielectric absorption. Yet most of them require specific pre-treatment prior to the microwave treatment. Here, a one-step method with metal-assisted microwave treatment is presented for converting the carbon materials into nano-graphite. The high temperature generated by sparking induced by the microwave radiation on fork-shape metal foils is a novel approach and has great potential to be increased when higher melting point metals are used.

2. Experimental

2.1. Materials and characterization methods

The thicknesses of the Cu (99.99% pure, MTI corporation) and Al (UHV Aluminum Foil from All-Foils Inc.) foils are 25 μm and 500 μm, respectively. The metal foils were cut with a knife into fork-like shape and rinsed with isopropyl alcohol (IPA). The fork-like shape is intended to induce sparking during microwave irradiation. Details of the shape are presented in the supplementary material. A molar ratio of 95% Ar and 5% H_2 is used as the reducing environment. The microwave radiation is generated from a conventional household microwave oven (Hamilton Beach 900 W, 2.54 GHz). The raw coal used in this study is from Powder River Basin, WY [43] and finely ground into sub-millimeter grains. All samples are sealed in 20 mL glass scintillation vials.

The microwave treated materials were characterized with Raman Spectroscopy, Scanning Electron Microscopy (SEM), and Transmission Electron Microscopy (TEM). Raman spectroscopy was conducted using a Snowy Range Instruments Raman spectrometer with a 532 nm diode-pumped solid-state laser. SEM images were acquired using a FEI Quanta 250 with a 20 keV beam. TEM images were acquired with a FEI Tecnai G20 FE-TEM/STEM using a 200 keV beam.

2.2. Converting procedure

In this work, the raw coal powders were pressed onto the metal foils. The samples were sealed in a controlled environment followed by the microwave irradiation. The microwave radiation induces sparking to generate high temperature when the fork-like shape metal foils are used. The microwave radiation continues for a certain period of time beyond the sparking stopped. More specifically, raw coal powder (0.6 mg) was loaded onto a prepared metal foil and firmly pressed onto the foil surface with a disposable plastic spatula. The powder covers approximately 1/3 of the area of the metal foil near the fork-shape region, as described as the shadowed regions in the inset of Fig. S1(a). Next, the sample is sealed in the desired environment. For the ambient environment condition, the sample was simply sealed in air. For the Ar (inert) and Ar/H_2 (reducing) environment the samples were placed into a glass jar with environment control. The glass jar was initially pumped down to 310 mbar, followed by the desired Ar or Ar/H_2 flow with one standard cubic feet per minute (SCFM) flow rate of gas under standard pressure and temperature conditions for 5 min. This process was repeated 3 times. The microwave radiation duration was varied from 3 min to 45 min.

3. Results and discussions

To convert the raw coal powder, the major factors are: (1) high temperature (sparking); (2) reducing environment (Ar/H_2); (3) catalyst (Cu); and (4) microwave radiation. Note that in the following discussion, for comparison purpose, the Raman spectra taken from the untreated raw coal, and from the sample with successful conversion are displayed in each panel in Fig. 1. Specifically, the untreated raw coal is shown as black curve; while the successful converted sample is shown as red. The successful converted sample is also the one shown in Fig. 2(a) with 15 min microwave treatment, sparking induced, Cu foils, and reducing environment (Ar/H_2). The effects from each major factor will be discussed with each panel in Fig. 1.

First, let us look at the effects of the sparking. Fig. 1(a) shows the Raman spectra measured on the successfully converted samples (with sparking), non-sparking samples, and untreated raw coal. For the non-sparking sample, the fork-shape Cu foil is replaced by a rectangular shaped (10 mm × 20 mm) Cu foil, which will not induce sparking. In Raman spectrum, D (∼1350 cm^{-1}) and G (∼1580 cm^{-1}) peaks originate from the sp^2 carbon materials, which are expected in the coal molecules. For samples with long range order, in addition to the D and G peaks, 2D (∼2700 cm^{-1}) and G′ (∼2450 cm^{-1}) peaks are also expected [44]. It is obvious in Fig. 1(a) that no 2D peak was observed for the non-sparking sample and the spectrum is almost identical to that of the untreated coal. It can be concluded here that the high temperature produced by the sparking is one of the key ingredients for the nano-graphite conversion.

Similarly, sparking induced by microwave treatment is also necessary to convert graphene oxide (GO) into high quality graphene [38]. In the previous work, the sparking was induced in the mildly reduced GO with a pre-annealing procedure prior to the microwave treatment. On the contrary, in this work, the coal powders with pre-annealing (300 °C for 1 h under Argon) did not exhibit sparking during the microwave irradiation. The Raman spectrum of this pre-annealed coal powders is similar to the non-sparking sample in Fig. 1(a). Alternatively, in this work, the sparking is provided by a fork-shape metallic Cu foil. The sparking only lasts for few seconds occurred within the first 180 s of microwave time, even the total microwave duration can be as long as 45 min. Detail sparking duration analysis is described in the supplementary material. The sparking ceased due to the melt down of the fork-shape part of the metal foil. The blunt shape of the foil after the melting prevents it from further inducing sparking. The melt down of Cu foils also indicates that the sparking appeared near the fork-shape regions can heat the Cu foil to the melting point, ∼1085 °C, within few seconds.

Second, three environments are tested: ambient, inert (Ar) and reducing (Ar/H_2) environments. Fig. 1(b) compares three samples with these three environments as well as the untreated raw coal. The two samples, inert environment (pure Ar) and ambient environment (air), exhibit no 2D peak, indicating that no long range ordered structure has formed. The sample treated in the inert environment (Ar) exhibits a similar Raman spectrum as that of the untreated coal. This infers that under the inert environment, the high temperature induced from the sparking does not alter the coal materials to have observable changes in its Raman spectra. On the contrary, the sample treated in the ambient environment exhibits weaker D and G bands in the Raman spectrum. It is possible that the amount of the aromatic structured carbon

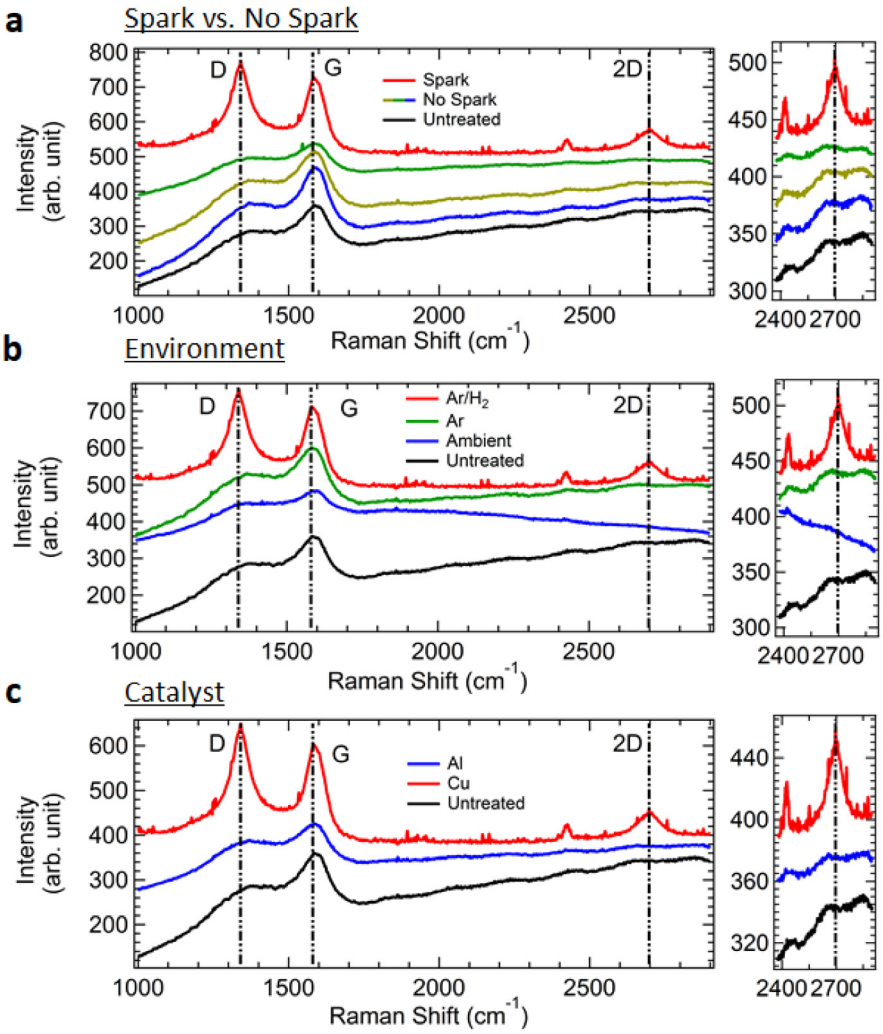

Fig. 1. Raman spectra taken on samples with various conditions. The spectra are grouped in the following ways to emphasis the effects from the major factors: (a) Sparking and non-sparking samples; (b) ambient, inert and reducing environments; (c) Cu (catalytic) and Al (non-catalytic) foils. In each plot, Raman spectra from untreated coal (black curves) and optimally converted samples (red curves) are added for comparison. (For interpretation of the references to color in this figure legend, the reader is referred to the web version of this article.)

materials is reduced after the sparking process. Coal combustion is likely taking place during the sparking process in the ambient condition. It is concluded that the reducing environment is a necessary factor for the conversion.

It was reported that H_2 could stabilize the C–H bonds at the edges of the graphite layers, preventing the formation of an amorphous carbon [45,46]. When converting very defective coal materials, the Ar/H_2 environment is needed to stabilize the edges to form larger size of crystalline graphite. Similarly, while dealing with complex carbon sources, such as food, insects, and waste, Ar/H_2 flow was used during the graphene synthesis phase [47], where Ar/H_2 flow serves as both the carrier gas as well as the reducing reagent for the complex carbon compounds. In our experiment, the Ar/H_2 is sealed in a vial, rather than flowing. It is possible that the flowing Ar/H_2 might produce better results, such as higher quantity or better quality of the nano-graphite. A microwave oven with tube passing through the microwave region is needed for this experiment. On the other hand, the conversion of GO to graphene through microwave treatment does not require the reduced environment. Only inert environment was used [38]. As GO is obtained by oxidizing graphite, GO has large basal plane structures with chemisorbed functional groups. The edge stabilization is not a key procedure to convert the GO back to graphene, hence the reducing environment is not critical.

Third, the importance of the catalytic role of Cu foil is tested. It is known that Fe, Co, and Ni are efficient catalysts for carbon nanotube (CNT) [48–51] and graphene [52–56] synthesis; while Cu [57], Ru [58], Ir [59], and Pt [60–62] have been used as catalytic substrates for graphene growth. On the other hand, Al is well known for its lack of catalytic activity for graphene growth [63]. Here, Al foil is used to replace Cu foil and the results are shown in Fig. 1(c). The Raman spectra taken on the samples treated with Al foil exhibit similar spectra as that of the untreated coal. This indicates that the Al foil does not facilitate the nano-graphite conversion from coal powder even with the sparking and the reducing environment. The Cu foil is required for the coal-to-nano-graphite conversion.

To wrap up with the Raman data presented in Fig. 1, the successful coal-to-nano-graphite conversion requires the following ingredients: (1) high temperature (sparking), (2) reducing environment (Ar/H_2), and (3) catalyst (Cu foil). In stark contrast with other synthesis methods, such as the CVD method, the high temperature here is generated by sparking that occurs during microwave radiation with fork shaped metal foils (see supplementary material). The advantage of this method is the cost effectiveness due to the low heating load. In general, the fast heating and cooling may be the key to induce the nano-particles [64]. Furthermore, higher temperatures may be attained

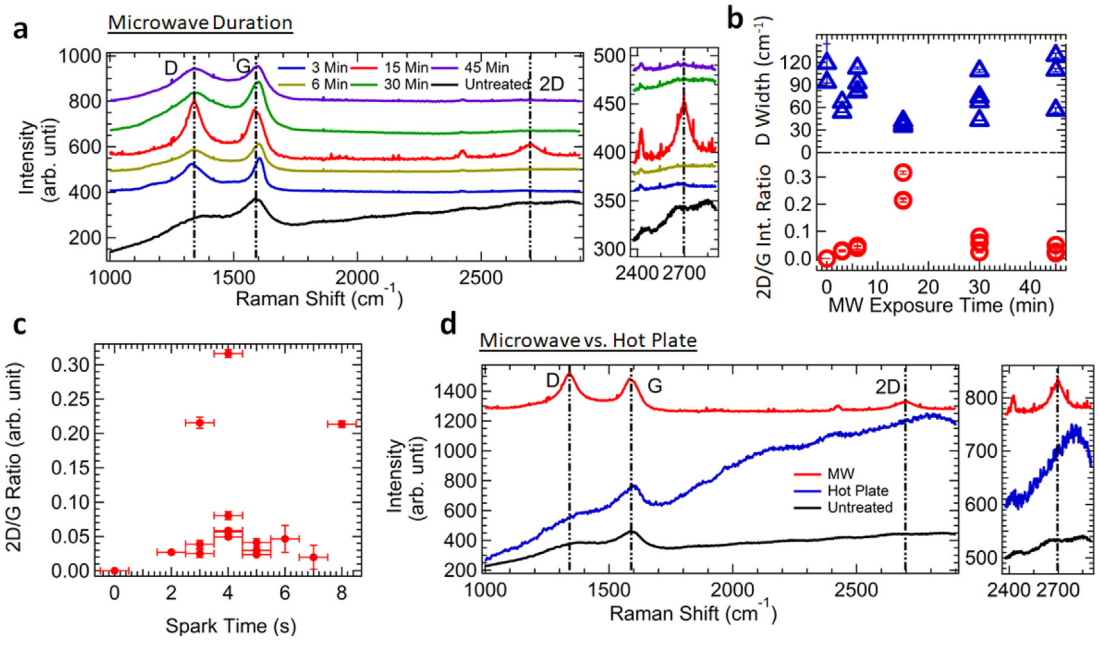

Fig. 2. Determining microwave duration effects. (a) Raman spectra of samples with various microwave exposure durations. (b) The D peak width, 2D/G intensity ratio as function of the microwave exposure durations. (c) 2D/G intensity ratio as function of the sparking time. (d) The Raman spectra of samples treated with 15-min microwave exposure as well as samples treated with 30 s microwave exposure (with sparking) followed by 14.5-minutes 400 °C hot plate heating.

with high-melting-point metal foils. It possibly widens the range of carbon materials to be produced with this method.

The additional factor that may affect the conversion is the microwave radiation duration. The Raman spectra taken on samples prepared with varying microwave exposure durations (ranging from 3 to 45 min) and the required factors (sparking, Ar/H_2, and Cu foil) are shown in Fig. 2(a). The 2D and G′ peaks are visible in all samples, indicating they all have successful conversion. Among them, the samples treated with 15 min of microwave radiation exhibit the sharpest D peak and highest 2D/G intensity ratio, as summarized in Fig. 2(b). This infers that the 15 min of microwave radiation (including the few seconds of sparking period in the first three minutes) shows the most significant conversion. One might argue that this observation could originate from the sparking duration, which is not fully controllable as the sparking in each trial only lasts for few seconds (see supplementary material). This is ruled out by Fig. 2(c), where the 2D/G intensity ratio versus sparking duration for each sample is plotted, where no correlation between the observed 2D/G ratio and the total sparking duration is observed. With these observations, in addition to the role of inducing sparking, the microwave radiation actively participates in the conversion of nano-graphite.

While the microwave radiation seems to be influencing the conversion, it is unclear whether the effects of the microwave radiation thermal or non-thermal. To distinguish the two scenarios, two samples were prepared. While the sparking, reducing environment, and Cu foils are identical for the two samples, the first sample undergoes a full 15 min of microwave radiation while the second sample is exposed to 0.5 min of microwave radiation (with sparking) followed by hot-plate annealed for another 14.5 min. In our setup, the temperature due to the microwave absorption (thermal effects) in the converted coal powder cannot be measured. It was reported that the maximum temperature attainable by microwave heating (2.455 GHz, 1.5 kW) for nano-scale graphite/carbon materials is only ∼200–500 °C [65]. In this work, the microwave oven used has a power of 900 W. It is estimated that the microwave heating in our converted coal samples will be near 400 °C or less. The Raman spectra of this hot plate treated sample and of the full 15-minute microwave treated sample are compared in Fig. 2(d). The Raman spectrum of the hot-plate treated sample shows no 2D peak nor a significant change in D and G peaks compared to that of the untreated coal, indicating no significant conversion has happened. The results further point out that the microwave treatment in the coal-to-nano-graphite conversion is not simply a thermal effect. The microwave radiation has non-thermal effects on the chemical reactions for the successful conversion.

The definitive evidence of the nano-graphite conversion comes from the high resolution TEM images and the selected area diffraction patterns. The sample used for TEM measurements is the optimally converted sample (sparking, Ar/H_2 environment, Cu foils, and 15 min of microwave treatment). Though the coal powder was firmly pressed prior to the microwave treatment, there are loose powders after the microwave treatment. The Raman measurements presented above were measured on the Cu foils after shaking off the loose powder. Thus, the materials of interest for TEM measurements were the materials on the Cu foils which were removed through gentle scraping and sonication. Fig. 3(a) and (b) are the selected area diffraction patterns measured on the raw coal powder and the crystalline regions of the converted samples. The radial average of the diffraction signal is plotted beneath the diffraction pattern for better visualization. Locations of the diffraction rings for graphite, CuO and Cu_2O are added as dashed and colored half-rings in the diffraction images. Vertical lines correlate the peak position to the rings observed in the diffraction pattern. Clearly the untreated coal has no sharp diffraction rings owing to the lack of long-range order. Also, the position of the broad peak does not match to any of the features from graphite, CuO or Cu_2O. On the contrary, the diffraction pattern from the successful converted sample (Fig. 3(b)) exhibits sharp and well-defined rings and dot-like features, which matched to the crystalline planes of graphite, CuO and Cu_2O [66]. The dot-like features indicate the products are closer to the polycrystalline case. The CuO and Cu_2O are possibly formed by either the oxygen in the raw coal or after the exposure to the air for Raman and TEM measurements. Fig. 3(c) shows the TEM images at the location where the diffraction pattern was collected. From a line profile taken at the path indicated as the

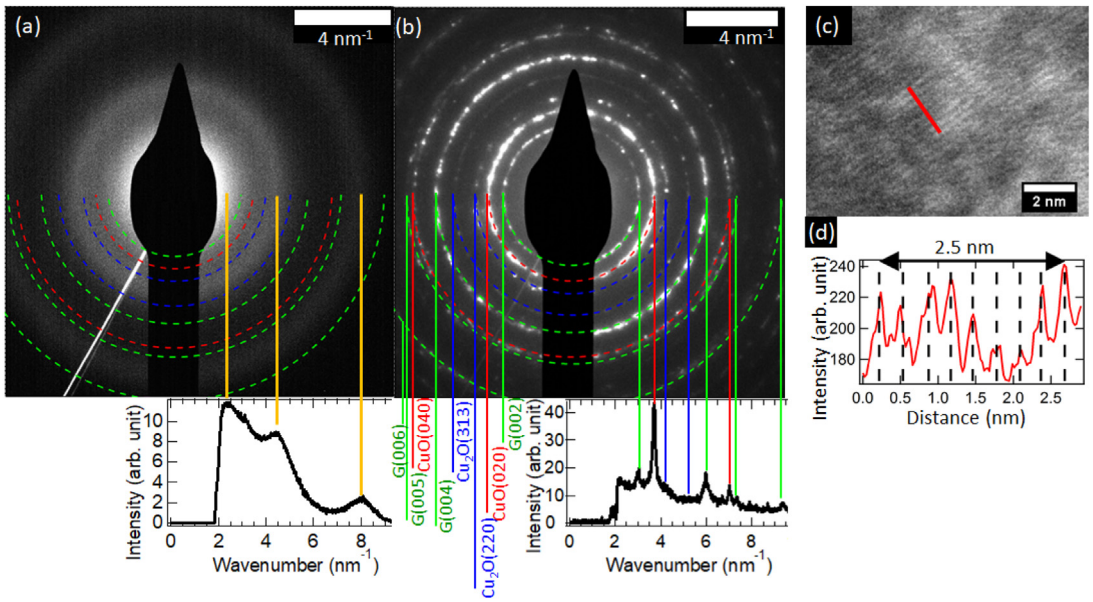

Fig. 3. TEM image and selected area diffraction of coal derived nano-graphite. (a) Diffraction pattern of the untreated coal with radial average beneath it. (b) Diffraction pattern of converted coal with radial average beneath it. The ring features match well with that of graphite, CuO and Cu_2O. (c) A TEM image shows the fringes where the selected area diffraction was measured. (d) Line profile from (c) measuring across 8 valleys for 2.5 ± 0.2 nm results in 0.31 ± 0.03 nm per fringe. (For interpretation of the references to color in this figure legend, the reader is referred to the web version of this article.)

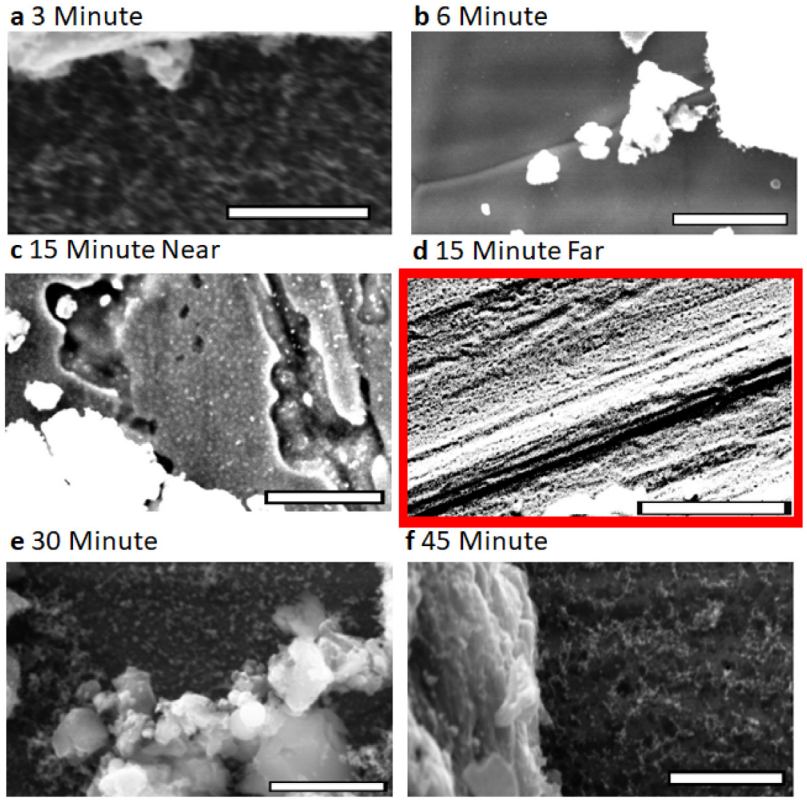

Fig. 4. SEM images of the five samples with various microwave treatment duration: (a) 3-min; (b) 6-min; (c), (d) 15-min; (e) 30-min; and (f) 45-min. All the SEM images were measured from the regions near the melted areas except (d), which was measured far away from the melted regions for comparison. The scale bar in each figure is 5 μm.

red solid line in Fig. 3(c), 2.5 ± 0.2 nm was measured across eight fringes, or 0.31 ± 0.03 nm per fringe. The results are comparable to the reported nano-graphite/Fe_3O_4 composited prepared from pure nano-graphite [67]. This is corresponding to the interlayer spacing of the graphite along the *c*-axis, hence the nano-graphite is determined.

Successful conversion occurs only for the carbon materials directly in contact with the Cu foil and adjacent to the sparking site. The surface morphology evolution as a function of the

microwave exposure duration is measured by scanning electron microscopy (SEM), as shown in Fig. 4. Except Fig. 4(d), all of the other SEM images presented were captured near the melted regions where nano-graphite was observed in the Raman spectra and TEM images. The morphology is observed to evolve from a rough surface (3-min sample, Fig. 4(a)), to smooth surface (6-min sample, Fig. 4(b)), to a smooth, thick surface (15-min sample, Fig. 4(c)), and back to a rough surface (30- and 45-min samples, Fig. 4(e) and (f)). Comparing with the Raman measurements, the smooth layers seen in SEM images for 6-min and 15-min cases are directly related to the polycrystalline nano-graphites. For the locations far away from the melted regions in the 15-min sample (Fig. 4(d)), the rough morphology is consistent with the observation in the TEM images of the samples with low or no conversion. This observation is consistent with the picture that the coal powder far away from the high temperature region (melted region) does not undergo the conversion.

Based on the observations described above, a working hypothetical mechanism for the conversion of nano-graphite from coal materials via metal assisted microwave treatment is postulated here. First, the high temperature produced by sparking initiates the process. Upon sparking, the coal powder adjacent to the sparking regions gain significant amount of thermal energy allowing for chemical bond breaking. Second, upon cooling, the catalytic role of Cu foil is essential to facilitate the formation of graphitic sp^2 bonding. Third, the hydrogen in reducing environment stabilizes the edge of the formed graphitic structure. And finally, the continuous microwave radiation further assists the conversion and growth in thickness through a non-thermal effect.

In fact, the formation of nano-graphite (multilayer graphene) is rather peculiar. It has been widely studied and accepted that only single layer graphene will be formed on Cu foils using CVD method. This is believed to be owing to the low solubility of carbon in the Cu. Therefore, it is expected here that only the single layer graphene will be produced. Thus, the formation of the nano-graphite shown indicates that the microwave treatment may play an important role in growing multilayer graphene (nano-graphite).

4. Conclusion

In summary, using Cu foil, a reducing environment, and a household microwave oven, the production of the nano-graphite material from raw coal powder has been successfully demonstrated. It is determined that the high temperature (by sparking), the catalyst (Cu foil), and the reducing environment (Ar/H_2), are essential for the conversion while the microwave radiation exhibits non-thermal effects that allow for the multilayer graphene growth. This method provides a new route to convert abundant carbon sources to high value materials with ecological and economic benefits. This method is also potentially applicable to the synthesis of the metal oxide powders [68–75].

CRediT authorship contribution statement

Christoffer A. Masi: Performed the synthesis, Characterizations, Manuscript preparation, Writing. **Teneil A. Schumacher:** Initiated the microwave experiments, Writing. **Joann Hilman:** Assisted in performing the SEM measurements, Writing. **Rabindra Dulal:** Assisted in performing the SEM measurements, Writing. **Gaurab Rimal:** Assisted in performing TEM measurements, Writing. **Bang Xu:** Prepared and provided the coal powder, Writing. **Brian Leonard:** Oversee the project, Writing. **Jinke Tang:** Oversee the project, Writing. **Maohong Fan:** Oversee the project, Writing. **TeYu Chien:** Oversee the project, Writing.

Declaration of competing interest

The authors declare that they have no known competing financial interests or personal relationships that could have appeared to influence the work reported in this paper.

Acknowledgment

This work is funded by the U.S. National Science Foundation, Division of Materials Research (DMR), USA (Grants No. DMR-1710512).

Appendix A. Supplementary data

Supplementary material related to this article can be found online at https://doi.org/10.1016/j.nanoso.2020.100660.

References

[1] E.I.A. Annual Coal Report, 2019.
[2] Y. Al-Douri, A.O. Basheer, Production of powder-activated carbon from natural resources, in: Nanoparticles in Analytical and Medical Devices, INC, 2021, pp. 277–299.
[3] C.-G. Lee, Y.-J. Hwang, Y.-M. Choi, J.-K. Lee, C. Choi, J.-M. Oh, A study on the tribological characteristics of graphite nano lubricants, Int. J. Precis. Eng. Manuf. 10 (2009) 85–90.
[4] D.D.L. Chung, Review exfoliation of graphite, J. Mater. Sci. 22 (1987) 4190–4198.
[5] R.A. Al-Samarai, A.S. Mahmood, Y. Al-Douri, Surface modification, including polymerization, nanocoating, and microencapsulation, in: Metal Oxide Powder Technologies, Vol. 2, INC, 2020, pp. 83–99.
[6] D.D.L. Chung, Electrical applications of carbon materials, J. Mater. Sci. 39 (2004) 2645–2661.
[7] J. Bai, X. Liao, E. Huang, Y. Luo, Q. Yang, G. Li, Control of the cell structure of microcellular silicone rubber/nanographite foam for enhanced mechanical performance, Mater. Des. 133 (2017) 288–298.
[8] Y. Sun, S. Wang, C. Li, P. Luo, L. Tao, Y. Wei, G. Shi, Large scale preparation of graphene quantum dots from graphite with tunable fluorescence properties, Phys. Chem. Chem. Phys. 15 (2013) 9907–9913.
[9] F. Liu, M.H. Jang, H.D. Ha, J.H. Kim, Y.H. Cho, T.S. Seo, Facile synthetic method for pristine graphene quantum dots and graphene oxide quantum dots: Origin of blue and green luminescence, Adv. Mater. 25 (2013) 3657–3662.
[10] M.S. Dresselhaus, G. Dresselhaus, New directions in intercalation research, Mol. Cryst. Liq. Cryst. 244 (1994) 1–12.
[11] B. Logan, S. Cheng, V. Watson, G. Estadt, Graphite fiber brush anodes for increased power production in air-cathode microbial fuel cells, Environ. Sci. Technol. 41 (2007) 3341–3346.
[12] L. Tonelli, L. Pezzato, P. Dolcet, M. Dabalà, C. Martini, Effects of graphite nano-particle additions on dry sliding behaviour of plasma-electrolytic-oxidation-treated EV31a magnesium alloy against steel in air, Wear 404–405 (2018) 122–132.
[13] K. Persson, Y. Hinuma, Y.S. Meng, A. Van derVen, G. Ceder, Thermodynamic and kinetic properties of the li-graphite system from first-principles calculations, Phys. Rev. B 82 (2010) 125416.
[14] R. Bhima Rao, N. Patnaik, Preparation of high pure graphite by alkali digestion method, Scand. J. Metall. 33 (2004) 257–260.
[15] S. Chehreh Chelgani, M. Rudolph, R. Kratzsch, D. Sandmann, J. Gutzmer, A review of graphite beneficiation techniques, Miner. Process. Extr. Metall. Rev. 37 (2016) 58–68.
[16] D.G. Levine, R.H. Schlosberg, B.G. Silbernagel, Understanding the chemistry and physics of coal structure (a review), Proc. Natl. Acad. Sci. 79 (1982) 3365–3370.
[17] W.H. Qu, Y.B. Guo, W.Z. Shen, W.C. Li, Using asphaltene supermolecules derived from coal for the preparation of efficient carbon electrodes for supercapacitors, J. Phys. Chem. C 120 (2016) 15105–15113.
[18] T.X. Phuoc, P. Wang, D. McIntyre, Detection of rare earth elements in powder river basin sub-bituminous coal ash using laser-induced breakdown spectroscopy (LIBS), Fuel 163 (2016) 129–132.
[19] B.J. Cardott, M.E. Curtis, Identification and nanoporosity of macerals in coal by scanning electron microscopy, Int. J. Coal Geol. 190 (2018) 205–217.
[20] L. Lu, V. Sahajwalla, C. Kong, D. Harris, Quantative X-ray diffraction analysis and its application to various coals, Carbon N. Y 39 (2001) 1821–1833.
[21] J.P. Mathews, A.L. Chaffee, The molecular representations of coal - a review, Fuel 96 (2012) 1–14.

[22] C. Xia, T. Wiltowski, S. Harpalani, Y. Liang, Coal depolymerization using permanganate under optimal conditions, Int. J. Coal Geol. 168 (2016) 214–221.
[23] L.S.K. Pang, A.M. Vassallo, M.A. Wilson, Fullerenes from coal, Nature 352 (480) (1991).
[24] K. Moothi, S.E. Iyuke, M. Meyyappan, R. Falcon, Coal as a carbon source for carbon nanotube synthesis, Carbon N. Y 50 (2012) 2679–2690.
[25] K. Williams, M. Tachibana, J. Allen, L. Grigorian, S.-C. Cheng, S.L. Fang, G.U. Sumanasekera, A.L. Loper, J.H. Williams, P.C. Eklund, Single-wall carbon nanotubes from coal, Chem. Phys. Lett. 310 (1999) 31–37.
[26] G.H. Taylor, J.D.F. Gerald, L. Pang, M.A. Wilson, Cathode deposits in fullerene formation - microstructural evidence for independent pathways of pyrolytic carbon and nanobody formation, J. Cryst. Growth 135 (1994) 157–164.
[27] L.S.K. Pang, M.A. Wilson, Nanotubes from coal, Energy Fuels 7 (1993) 436–437.
[28] R. Ye, C. Xiang, J. Lin, Z. Peng, K. Huang, Z. Yan, N.P. Cook, E.L.G. Samuel, C.-C. Hwang, G. Ruan, et al., Coal as an abundant source of graphene quantum dots, Nat. Commun. 4 (2013) 2943.
[29] B.D. Keller, N. Ferralis, J.C. Grossman, Rethinking coal: Thin films of solution processed natural carbon nanoparticles for electronic devices, Nano Lett. 16 (2016) 2951–2957.
[30] E.T. Thostenson, T.-W. Chou, Microwave processing: Fundamentals and applications, Compos. Part A 30 (1999) 1055–1071.
[31] N.G. Cutmore, T.G. Evans, A.J. McEwan, C.A. Rogers, S.L. Stoddard, Low frequency microwave technique for on-line measurement of moisture, Miner. Eng. 13 (2000) 1615–1622.
[32] D.G. Ponte, I.F. Prieto, P.F. Viar, J.C.G. Luengo, Determination of moisture content in power station coal using microwaves, Fuel 75 (1996) 133–138.
[33] R.M. Perkin, The heat and mass transfer characteristics of boiling point drying using radio frequency and microwave electromagnetic fields, Int. J. Heat Mass Transf. 23 (1980) 687–695.
[34] N. Standish, H.K. Worner, H.R. Kaul, Microwave drying of brown coal agglomerates, J. Microw. Power Electromagn. Energy 23 (1988) 171–175.
[35] S. Marland, B. Han, A. Merchant, N. Rowson, The effect of microwave radiation on coal grindability, Fuel 79 (2000) 1283–1288.
[36] E. Lester, S. Kingman, The effect of microwave pre-heating on five different coals, Fuel 83 (2004) 1941–1947.
[37] M.S. Seehra, A. Kalra, A. Manivannan, Dewatering of fine coal slurries by selective heating with microwaves, Fuel 86 (2007) 829–834.
[38] D. Voiry, J. Yang, J. Kupferberg, R. Fullon, C. Lee, H.Y. Jeong, H.S. Shin, M. Chhowalla, High-quality graphene via microwave reduction of solution-exfoliated graphene oxide, Science 353 (2016) 1413–1416.
[39] X. Ma, M. Zhang, F. Min, Study of enhanced low-quality coal oxidative desulphurization and deashing by using HNO_3 and microwave pretreatment, Environ. Technol. 35 (2014) 36–41.
[40] S. Singh, V.B. Neculaes, V. Lissianski, G. Rizeq, S.B. Bulumulla, R. Subia, J. Manke, Microwave assisted coal conversion, Fuel 140 (2015) 495–501.
[41] H. Zhu, X. Wang, Y. Li, Z. Wang, F. Yang, X. Yang, Microwave synthesis of fluorescent carbon nanoparticles with electrochemiluminescence properties, Chem. Commun. (2009) 5118–5120.
[42] L. Tang, R. Ji, X. Li, K.S. Teng, S.P. Lau, Size-dependent structural and optical characteristics of glucose-derived graphene quantum dots, Part. Part. Syst. Charact. 30 (2013) 523–531.
[43] N.E.T. Laboratory, Quality Guidelines for energy system studies detailed: detailed coal specifications, 2019, October 2019.
[44] T. Shimada, T. Sugai, C. Fantini, M. Souza, L.G. Cançado, A. Jorio, M.A. Pimenta, R. Saito, A. Grüneis, G. Dresselhaus, et al., Origin of the 2450 cm^{-1} Raman bands in HOPG, single-wall and double-wall carbon nanotubes, Carbon N. Y 43 (2005) 1049–1054.
[45] P.E. Nolan, M.J. Schabel, D.C. Lynch, A.H. Cutler, Hydrogen control of carbon deposit morphology, Carbon N. Y 33 (1995) 79–85.
[46] V. Ivanov, J.B. Nagy, P. Lambin, A. Lucas, X.B. Zhang, X.F. Zhang, D. Bernaerts, G. VanTendeloo, S. Amelinckx, J. VanLanduyt, The study of carbon nanotubes produced by catalytic method, Chem. Phys. Lett. 223 (1994) 329–335.
[47] G. Ruan, Z. Sun, Z. Peng, J.M. Tour, Growth of graphene from food, insects and waste, ACS Nano 5 (2011) 7601–7607.
[48] A. Thess, R. Lee, P. Nikolaev, H. Dai, P. Petit, J. Robert, C. Xu, YH. Lee, SG. Kim, AG. Rinzler, D.T. Colbert, G.E. Scuseria, D. Tománek, J.E. Fischer, R.E. Smalley, Crystalline ropes of metallic carbon nanotubes, Science 273 (1996) 483–488.
[49] C. Journet, W.K. Maser, P. Bernier, A. Loiseau, M. Lamy de la Chapelle, S. Lefrant, P. Deniard, R. Lee, J.E. Fischer, Large-scale production of single-walled carbon nanotubes by the electric-arc technique, Nature 388 (1997) 756–758.
[50] S. Amelinckx, X.B. Zhang, D. Bernaerts, X.F. Zhang, V. Ivanov, J.B. Nagy, A formation mechanism for catalytically grown helix-shaped graphite nanotubes, Science 265 (1994) 635–639.
[51] K. Hernadi, A. Fonseca, J.B. Nagy, D. Bernaerts, A.A. Lucas, Fe-catalyzed carbon nanotube formation, Carbon N. Y 34 (1996) 1249–1257.
[52] A. Reina, X. Jia, J. Ho, D. Nezich, H. Son, V. Bulovic, M.S. Dresselhaus, J. Kong, Large area, few-layer graphene films on arbitrary substrates by chemical vapor deposition, Nano Lett. 9 (2009) 30–35.
[53] K.S. Kim, Y. Zhao, H. Jang, S.Y. Lee, J.M. Kim, K.S. Kim, J.H. Ahn, P. Kim, J.Y. Choi, B.H. Hong, Large-scale pattern growth of graphene films for stretchable transparent electrodes, Nature 457 (2009) 706–710.
[54] Q. Yu, J. Lian, S. Siriponglert, H. Li, Y.P. Chen, S.S. Pei, Graphene segregated on Ni surfaces and transferred to insulators, Appl. Phys. Lett. 93 (2008) 113103.
[55] D. Kondo, S. Sato, K. Yagi, N. Harada, M. Sato, M. Nihei, N. Yokoyama, Low-temperature synthesis of graphene and fabrication of top-gated field effect transistors without using transfer processes, Appl. Phys. Express 3 (2010) 025102.
[56] H. Ago, Y. Ito, N. Mizuta, K. Yoshida, B. Hu, C.M. Orofeo, M. Tsuji, K. Ikeda, S. Mizuno, Epitaxial chemical vapor deposition growth of single-layer graphene over, ACS Nano 4 (2010) 7407–7414.
[57] X. Li, W. Cai, J. An, S. Kim, J. Nah, D. Yang, R. Piner, A. Velamakanni, I. Jung, T. Emanuel, et al., Large area synthesis of high-quality and uniform graphene films on copper foils, Science 324 (2009) 1312–1314.
[58] P.W. Sutter, J.I. Flege, E.A. Sutter, Epitaxial graphene on ruthenium, Nat. Mater. 7 (2008) 406–411.
[59] J. Coraux, A.T. N'Diaye, C. Busse, T. Michely, Structural coherency of graphene on Ir(111), Nano Lett. 8 (2008) 565–570.
[60] B.J. Kang, J.H. Mun, C.Y. Hwang, B.J. Cho, Monolayer graphene growth on sputtered thin film platinum, J. Appl. Phys. 106 (2009) 104309.
[61] H. Ueta, M. Saida, C. Nakai, Y. Yamada, M. Sasaki, S. Yamamoto, Highly oriented monolayer graphite formation on Pt(111) by a supersonic methane beam, Surf. Sci. 560 (2004) 183–190.
[62] D.E. Starr, E.M. Pazhetnov, A.I. Stadnichenko, A.I. Boronin, S.K. Shaikhutdinov, Carbon films grown on Pt(111) as supports for model gold catalysts, Surf. Sci. 600 (2006) 2688–2695.
[63] S.F. Bartolucci, J. Paras, M.A. Rafiee, J. Rafiee, S. Lee, D. Kapoor, N. Koratkar, Graphene–aluminum nanocomposites, Mater. Sci. Eng. A 528 (2011) 7933–7937.
[64] Y. Al-Douri, S.A. Abdulateef, A.A. Odeh, C.H. Voon, N. Badi, Gano colloidal nanoparticles synthesis by nanosecond pulsed laser ablation: Laser fluence dependent optical absorption and structural properties, Powder Technol. 320 (2017) 457–461.
[65] K. Kashimura, S. Suzuki, M. Hayashi, T. Mitani, N. Shinohara, K. Nagata, Surface-plasmon-like modes of graphite powder compact in microwave heating, J. Appl. Phys. 112 (2012) 034905.
[66] J. Hilman, A.J. Yost, J. Tang, B. Leonard, T. Chien, Low temperature growth of cuo nanowires through direct oxidation, Nano-Struct. Nano-Objects 11 (2017) 124–128.
[67] C. Li, Y. Dong, J. Yang, Y. Li, C. Huang, Modified nano-graphite/Fe_3O_4 composite as efficient adsorbent for the removal of methyl violet from aqueous solution, J. Mol. Liq. 196 (2014) 348–356.
[68] Y.A. Wahab, S. Fatmadiana, M.N. Naseer, M.R. Johan, N.A. Hamizi, S. Sagadevan, O. Akbarzadeh, Z.Z. Chowdhury, T. Sabapathy, Y. AlDouri, Metal oxides powder technology in dielectric materials, in: Metal Oxide Powder Technologies, INC, 2020, pp. 385–399.
[69] W.K. Ahmed, Y. Al-Douri, Three-dimensional printing of ceramic powder technology, in: Metal Oxide Powder Technologies, INC, 2020, pp. 351–383.
[70] A.A. Odeh, Y. Al-Douri, Metal oxides in electronics, in: Metal Oxide Powder Technologies, INC, 2020, pp. 263–278.
[71] A.S. Mahmood, R.A. Al-Samarai, Y. Al-Douri, Metal oxides powder technology in energy technologies, in: Metal Oxide Powder Technologies, INC, 2020, pp. 253–262.
[72] A.O. Basheer, Y. Al-Douri, Z.Z. Chowdhury, Chemical processes of metal oxide powders, in: Metal Oxide Powder Technologies, INC, 2020, pp. 189–208.
[73] F. Ahmad, Y. Al-Douri, D. Kumar, S. Ahmad, Metal-oxide powder technology in biomedicine, in: Metal Oxide Powder Technologies, INC, 2020, pp. 121–168.
[74] Y. Al-Douri, Y.A. Wahab, N.A. Hamizi, Physical studies of metal oxide powders, in: Metal Oxide Powder Technologies, INC, 2020, pp. 1–15.
[75] C.H. Voon, K.L. Foo, B.Y. Lim, S.C.B. Gopinath, Y. Al-Douri, Synthesis and preparation of metal oxide powders, in: Metal Oxide Powder Technologies, INC, 2020, pp. 31–65.